Lef1 expression in fibroblasts maintains developmental potential in adult skin to regenerate wounds

Quan M. Phan[1], Gracelyn Fine[1], Lucia Salz[1], Gerardo G. Herrera[1], Ben Wildman[1], Iwona M. Driskell[1], and Ryan R. Driskell[1,2*]

[1]School of Molecular Biosciences, Washington State University, Pullman, WA

[2]Center for Reproductive Biology, Washington State University, Pullman, WA

[*] Corresponding Author: ryan.driskell@wsu.edu

Summary

Scars are a serious health concern that impacts the clinical outcome and long-term well-being of burn victims and individuals with genetic skin conditions associated with wound healing. In this study we identify regenerative factors in neonatal skin that will transform adult skin to regenerate instead of repairing wounds with a scar, without perturbing normal development and homeostasis. We utilized single-cell RNA-sequencing (scRNA-seq) to probe unsorted cells from Regenerating, Scarring, Homeostatic, and Developing skin. Our results revealed a transient regenerative cell type in Developing skin, called papillary fibroblasts, which are defined by the expression of a canonical Wnt transcription factor Lef1. Tissue specific ablation of Lef1 inhibited skin regeneration. Importantly, ectopic expression of Lef1 in dermal fibroblasts did not disrupt development and aging, but primed adult skin to undergo enhanced regeneration. In conclusion, we reveal the possibility of transferring the regenerative abilities of neonatal skin to adult tissue by expressing Lef1 in dermal fibroblasts. Finally, we have generated a web resource with a search function to display gene expression in the context of our scRNA-seq data (https://skinregeneration.org/).

Main

Understanding how to induce skin regeneration instead of scarring will have broad implications clinically and cosmetically (Walmsley et al., 2015). One of the main characteristics of scars is the absence of hair follicles, indicating that their regeneration in a wound may be a critical step in achieving scar-less skin repair (Yang and Cotsarelis, 2010). Interestingly, human embryonic skin has the capacity to regenerate without scars (Lo et al., 2012). Similarly, neonatal and adult mouse skin has the capacity to regenerate small non-functional hair follicles under specific conditions (Figure 1c-d)(Ito et al., 2007; Rognoni et al., 2016; Telerman et al., 2017) . These insights have prompted efforts in the field to define the molecular triggers that promote hair development in skin, with the ultimate goal of devising a way to regenerate fully functional hairs in adult skin wounds as a therapeutic modality (Yang and Cotsarelis, 2010).

Human and mouse skin are similar in their overall structural complexity, indicating that mouse skin can be a useful model to study skin development and wound repair (Chen et al., 2013). Murine hair follicle and skin development primarily occurs between embryonic day 12.5 (E12.5) to post-natal day 21 (P21) (Muller-Rover et al., 2001). During this time different fibroblast lineages are established that respond to the changes in the environment to support hair follicle and skin development (Driskell et al., 2013; Jiang et al., 2018; Rinkevich et al., 2015; Rognoni et al., 2016). Fibroblasts that support hair follicle development differentiate from the papillary fibroblast lineage, into dermal papilla (DP), dermal sheath (DS), and arrector pili (AP) cells (Driskell et al., 2013; Plikus et al., 2017). Reticular fibroblasts, which cannot differentiate into papillary fibroblast lineages, secrete Extra-Cellular-Matrix and form into adipocytes (Driskell et al., 2013; Schmidt and Horsley, 2013). By post-natal day 2 (P2) fibroblast heterogeneity is fully established with the presence of the defined layers of the dermis (Figure 1a)(Driskell et al., 2013). Skin maturation occurs after P2 with the formation of the AP and the completion of the first hair follicle cycle, which results in the loss of a defined papillary fibroblast layer (Figure 1b) (Driskell et

54 al., 2013; Rognoni et al., 2016; Salzer et al., 2018). We have previously shown that papillary
55 fibroblasts are the primary source of de-novo dermal papilla during skin development, which are
56 required for hair formation (Driskell et al., 2013). Furthermore, it has been suggested that adult
57 murine skin form scars due to the lack of a defined papillary layer (Driskell et al., 2013; Driskell
58 and Watt, 2015). Consequently, expanding this layer in adult skin might support skin regeneration
59 in adult mice.

60 The use of scRNA-seq in the murine skin has established useful cell atlases of the skin
61 during development and homeostasis (Guerrero-Juarez et al., 2019; Haensel et al., 2020; Joost
62 et al., 2020; Joost et al., 2018; Joost et al., 2016; Mok et al., 2019). In addition, scRNA-seq studies
63 investigating wound healing have so far focused on comparing scarring, non-scarring, or
64 regenerating conditions (Guerrero-Juarez et al., 2019; Haensel et al., 2020; Joost et al., 2018).
65 These studies have helped to identified key markers of the newly discovered skin fascia, such as
66 Gpx3, which recently has been shown to contribute to scar formation (Correa-Gallegos et al.,
67 2019; Grachtchouk et al., 2000; Joost et al., 2020). These, scRNA-seq studies have revealed that
68 transgenic activation of the Shh pathway in the alpha-smooth-actin cells in scarring wounds,
69 which includes pericytes, blood vessels, and myo-fibroblasts, can support small non-functional
70 hair regeneration (Lim et al., 2018). However, activation of Shh pathway in dermal fibroblasts is
71 associated with malignant phenotypes and will perturb development and homeostasis such that
72 it may not be a safe target to support human skin regeneration clinically (Fan et al., 1997;
73 Grachtchouk et al., 2000; Oro et al., 1997; Sun et al., 2020). Altogether, these findings suggest
74 that an overall comparison of developing, homeostatic, scarring, and regenerating skin conditions
75 will yield important discoveries for molecular factors that can safely support skin regeneration
76 without harmful side effects.

77 The Wnt signaling pathway is involved in regulating development, wound healing, disease
78 and cancer (Nusse and Clevers, 2017). Studies that activated Wnt and β-catenin in skin have led

79 to important discoveries for wound healing but have produced contrasting results in the context
80 of fibroblast biology and hair follicle formation (Chen et al., 2012; Enshell-Seijffers et al., 2010;
81 Hamburg-Shields et al., 2015; Lim et al., 2018; Rognoni et al., 2016). Wnt is a secreted protein
82 that activates a cascade of events that stabilizes nuclear β-catenin, which operates as a powerful
83 co-transcription factor of gene expression. Importantly, β-catenin along cannot activate the
84 expression of Wnt target genes without co-transcription factors. There are four Wnt co-
85 transcription factors Tcf1 (Tcf7), Lef1, Tcf3 (Tcf7l2), and Tcf4 (Tcf7l2). These co-transcription
86 factors modulate the functional outcome of Wnt signaling by binding to different target genes
87 (Adam et al., 2018; Nguyen et al., 2009; Yu et al., 2012). In the context of wound healing and
88 regeneration, it is not known how differential expression of Tcf/Lef can modulate fibroblast activity
89 via Wnt signaling.

90 Since it has been shown that embryonic and neonatal skin have the potential to regenerate
91 in a scar-less fashion (Hu et al., 2018; Rognoni et al., 2016), we set out to identify the cell types
92 and molecular factors that define this ability in order to transfer this regenerative potential to adult
93 tissue. Our work has identified Lef1, as the factor in fibroblast of developing skin, that can
94 transform adult tissue to regenerate without harmful phenotypes.

95 **Developing papillary fibroblasts are a transient cell population that supports hair follicle**
96 **regeneration in wounds**

97 We and others have previously shown that there are differences between neonatal and
98 adult skin in terms of their cellular and biological properties (Ge et al., 2020; Rognoni et al., 2016;
99 Salzer et al., 2018). These differences influence how skin can repair or if it can regenerate hair
100 follicles in a wound. We showed that neonatal Developing skin at P2 (Figure 1a) can regenerate
101 small hair follicles 7 days after wounding (7dpw) (Figure 1c), while adult Homeostatic skin at P21
102 (Figure 1b) heals by scarring 7dpw (Figure 1d). Consequently, we hypothesized that Developing
103 or Regenerating skin contains cell types that are distinct and will support hair follicle reformation

104 in wounds. In order to identify the cell types and molecular pathways that define the ability of
105 Developing skin to regenerate we performed a comparison of unsorted cells from 4 conditions
106 using scRNA-seq (Figure 1e). We generated sequencing libraries of the 66,407 cells that could
107 be distinguished between each condition by UMAP plotting as different colors (Figure 1f) (see
108 methods Github weblink). UMAP plotting of the 66,407 sequenced cells revealed distinct clusters
109 (Figure 1f-g). To identify cell clusters, we used Louvain modulating analysis (Joost et al., 2016;
110 Wolf et al., 2018), which resulted in 18 distinct clusters (Figure 1g). We assigned 7 main classes
111 of cells to the clusters. Keratinocytes represented the largest portion of cell types in the analysis
112 (blue clusters - 0,1,2,5,8,9,11,12,17) (Figure 1h). We identified three distinct fibroblast clusters
113 (green clusters -3,4,16). These clusters expressed Twist2/Dermo1, Pdgfra, and En1 (Figure 1h).
114 We also identified other clusters based on their distinct gene expression profile (Figure 1h), such
115 as immune cells (cluster 6), vasculature (cluster 7, 15), Schwann cells (cluster 10), melanocytes
116 (cluster 13), and a pericyte populations (cluster 14).

117 To identify a unique cell type that supports the ability to regenerate hair follicles in
118 Developing skin we quantified the number of cells for each condition within a cluster (Figure 1i).
119 Unexpectedly there was no cluster defined by the Regenerating condition. Regenerating (green)
120 and Scarring (red) conditions were found in similar proportions amongst Keratinocytes,
121 lymphocytes/blood, melanocytes, Schwann cells, blood vessels and fibroblasts (Figure 1i). There
122 were two clusters that were distinct based on the representation of cell types from a specific
123 condition. Cluster 16 consisted of 99.9% of fibroblasts from Homeostatic skin, while Cluster 3
124 consisted of 67.8% of Developing fibroblasts (Figure 1i). In addition, cluster 4 consisted of 25.7%
125 of Regenerating condition, 57.6% of the Scarring conditions. Since fibroblasts are known to play
126 a critical (crucial) role in regulating hair follicle reformation in wounds by differentiating into de-
127 novo DP (Driskell et al., 2013; Plikus et al., 2017; Rognoni et al., 2016), we further analyzed
128 clusters 3,4,and 16.

129 We subset the fibroblast clusters 3,4,16 and re-clustered them by performing an
130 integration analysis (Polanski et al., 2020). This allowed us to test if different fibroblast subtypes,
131 such as the papillary and reticular/hypodermal/fascia lineages, would be represented uniquely
132 within a condition (Figure 1j-l). UMAP plotting of the integrated analysis and Louvain clustering
133 revealed 10 distinct clusters (Figure 1k). The largest cluster (cluster 0) expressed markers of the
134 papillary fibroblast lineage (Figure 1e-g). Four clusters (clusters 1,2,3,4) distinctly expressed
135 markers of the reticular/hypodermal/fascia layers of the dermis (Figure 1k; Supp Fig 1a) (Correa-
136 Gallegos et al., 2019; Joost et al., 2018). Three clusters (clusters 6,7,8) expressed markers of the
137 dermal papilla and dermal sheath (Figure 1e-g). One cluster was distinctly represented by alpha-
138 smooth-muscle actin indicating a myofibroblast subtype (cluster 9).

139 To identify the type of condition that is represented within specific fibroblast subtypes, we
140 quantified the percentage of cells from each condition within the sub-clusters (Figure 1l). Our
141 results revealed that four clusters were uniquely represented by four conditions. The
142 myofibroblast sub-cluster (cluster 9) contained 69% of cells from the Regenerating condition,
143 while a hypodermal fascia cluster (cluster 1) contained 92.2% of cells from the Scarring condition.
144 Cluster 4, identified by the high expression of Cochlin (Coch), an inner ear ECM protein, contained
145 80.8% of cells from the Homeostasis condition and a DP/DS sub-clusters (cluster 6) contained
146 95.0% of cells from the Homeostasis condition. The papillary fibroblast cluster (cluster 0)
147 contained 98.1% of cells from the Developing skin condition. The DP sub-cluster (cluster 7)
148 consisted of 56.5% cells from the Developing condition and 37.1% cells from the Regenerating
149 condition. These results indicate that there is a distinct separation between fibroblast sub-types
150 that support regeneration (papillary fibroblast) or scarring (reticular/hypodermal/fascia) based on
151 conditions.

152 In homeostatic skin DP and DS are critical for hair follicle growth and cycling. However,
153 they do not migrate into wounds to support hair follicle reformation (Johnston et al., 2013; Kaushal

154 et al., 2015). Myofibroblasts migrate into wounds but have not been shown to differentiate into
155 dermal papilla during hair follicle regeneration and is a major characteristic of scarring (Lim et al.,
156 2018; Plikus et al., 2017). Furthermore, reticular and fascia fibroblasts contribute to scar
157 formation but not differentiate into dermal papilla (Correa-Gallegos et al., 2019; Driskell et al.,
158 2013). Since our goal was to identify a cell type that uniquely represented the ability to support
159 hair follicle regeneration in wounds, we focused on cluster 0 which are papillary fibroblasts
160 represented by the Regenerating condition. Papillary fibroblasts migrate into wounds and support
161 the reformation of hair follicles by differentiating into dermal papilla (Driskell et al., 2013; Rognoni
162 et al., 2016). We conclude that the papillary fibroblasts found only in the Developing condition are
163 unique and might harbor the potential to support hair follicle regeneration in wounds.

164 **Lef1 drives the papillary lineage trajectory in Developing fibroblasts**

165 We have previously identified molecular markers of papillary, reticular and hypodermal
166 fibroblasts in Developing P2 skin (Driskell et al., 2013). P2 developing skin is a critical time point
167 to study the regenerative properties that can be transferrable to adult tissue. Consequently, we
168 have generated a web-resource for this time point (https://skinregeneration.org/). Dpp4/CD26
169 marks the papillary fibroblast region with the highest expression with detectable signal in the
170 reticular layer, which expresses high levels of Dlk1/Pref1 (Figure 2a-b). The hypodermis is co-
171 labeled with Dlk1/Pref1 and Ly6a/Sca1 expression (Figure 2b-c). We subset and re-clustered the
172 Developing P2 fibroblasts to generate a UMAP to produce a cell atlas in the context of previously
173 defined markers of fibroblast heterogeneity (Figure 2d). Importantly, we found that PDGFRa, a
174 pan fibroblast marker, was expressed in all populations (Figure 2d) (Collins et al., 2011).
175 Dlk1/Pref1 and Ly6a/Sca1 labeled clusters above a population that expressed the newly identified
176 fascia marker Gpx3 (Figure 2d). Dpp4/CD26 was detected above the Dlk1/Pref1 clusters. Dkk1,
177 a newly identified papillary marker (Rognoni et al., 2016), was expressed in an adjacent
178 population to the Dpp4/CD26 population. MKi67 marked cells undergoing division, but importantly

179 overlapped with Dpp4/CD26 and Dkk1 expression, suggesting that this cluster represented
180 dividing papillary fibroblasts. Acan, a newly identified DS marker (Heitman et al., 2020), was
181 detected in a small population adjacent to the cluster which expressed the DP marker Corin
182 (Enshell-Seijffers et al., 2008). We conclude that our scRNA-seq analysis of Developing
183 fibroblasts supports previously identified markers defining fibroblast lineages but expose the
184 existence of two papillary fibroblast populations, suggesting additional heterogeneity to be
185 investigated in future studies.

186 To identify factors that define the papillary fibroblast clusters we performed an RNA
187 Velocity analysis on Developing fibroblasts (Figure 2e) (Methods: Github weblink). RNA Velocity
188 is a function of scRNA-seq that computationally compares the ratio of spliced/unspliced mRNA
189 sequencing data, within a cell, to establish an estimated trajectory of differentiation, projected as
190 arrows on a UMAP plot (Figure 2e) (La Manno et al., 2018). The arrows are defined by a list of
191 driver genes (Supp Table 1). Interestingly, the estimated trajectories of the clusters support our
192 previous work indicating that cells that express Ly6a/Sca1 do not differentiate into the papillary
193 lineage (Driskell et al., 2013). We probed the list of Velocity driver genes (Supp Table 2) using
194 GO Pathway analysis (Figure 2f). The Wnt signaling pathway was one of the most significant
195 pathways represented. RNA Velocity analysis also ranks the top 5 drivers for each cluster, which
196 revealed two canonical Wnt transcription factors with opposing trajectories (Figure 2g-h). Lef1,
197 driving trajectories of 2 papillary clusters and Tcf4 driving the hypodermal cluster. Importantly,
198 Lef1 is an early DP marker capable of enhancing human hair follicle growth in vitro, while Tcf4 is
199 associated with fibrotic scars (Mok et al., 2019)(https://doi.org/10.1101/2020.01.05.895334). We
200 projected the velocity of Lef1 and Tcf4 as gradients of color on UMPAs of Developing fibroblasts
201 (Figure 2h) to visualize the direction of their trajectories. The velocity of Lef1 was positive in the
202 direction of all papillary clusters including the dermal papilla and dermal sheath. Tcf4 velocity was
203 positive toward the reticular/hypodermal/fascia clusters. To validate Lef1 expression in papillary

204 fibroblasts, we immunostained Developing (P2) and Homeostatic (P21) tissue samples (Figure
205 2i-l). We found Lef1 expression in the papillary region of Developing skin, which was lost in adult
206 dermis and correlates with the loss of regenerative ability in Homeostatic skin. Likewise, we
207 confirmed that Tcf4 was detected in the reticular/hypodermis throughout Developing skin and in
208 Homeostasis but not in papillary fibroblasts. Interestingly, it has been previously shown that the
209 response to Wnt signals could be specified by the different Tcf factors expressed (Adam et al.,
210 2018). Since Lef1 has previously been defined as an early DP marker (Mok et al., 2019) we
211 hypothesize that Lef1 marks papillary fibroblasts capable of supporting hair follicle regeneration
212 in wounds.

213 **Neonatal skin regeneration requires Lef1 expression in fibroblasts**

214 Based on our scRNA-seq findings, we hypothesized that Lef1 defines a neonatal papillary
215 fibroblast that supports skin regeneration during neonatal wound healing. To test if Lef1 in
216 fibroblasts is required to support neonatal regeneration, we produced a tissue specific knockout
217 model. We utilized the fibroblast specific promoter Dermo1/Twist2 to drive Cre expression, bred
218 with a mouse line with flox sites flanking Exon 7 and 8 of the Lef1 locus (Yu et al., 2012). We
219 called this mouse line DermLef1KO (Figure 3a). DermLef1KO mice were viable and fertile with
220 small shifts in hair follicle phenotypes that resulted in less dense fur (Manuscript in Prep). We
221 confirmed dermal Lef1 ablation from the papillary fibroblast at P2 and from adult DP by
222 immunostaining (Figure 3b-e). We also performed 2mm wounds on P2 DermLef1KO and wild
223 type littermates harvesting at 7dpw (Figure 3f). Our analyses revealed that Lef1 was expressed
224 in the de-novo DP and regenerating hair follicle buds of wild type mice (Figure 3g,i), but that
225 wounded DermLef1KO mice lacked regeneration (Figure 3h,j,k). We conclude that Lef1
226 expression in neonatal fibroblasts is required for hair follicle regeneration in wounds.

227 **Dermal Lef1 expression primes adult skin to enhance regeneration in large wounds**

228 Our scRNA-seq data, together with tissue specific knockout, suggests that skin can be
229 primed to regenerate during development and homeostasis. We hypothesize that constitutively
230 active Lef1 expression in dermal fibroblasts will prime skin to support regeneration. To induce
231 Lef1 expression in fibroblasts, we utilized a previously published transgenic mouse model Lef1KI
232 (Lynch et al., 2016) bred with Dermo1/Twist2-Cre mouse line called the DermLef1KI line (Figure
233 4a). We verified that Lef1 was expressed in all dermal fibroblast compartments in DermLef1KI
234 mice during development and in adult homeostatic skin conditions (Figure 4b-e). Importantly, the
235 only phenotype detected was the early entry of the hair follicle cycling into anagen at P21 in
236 DermLef1KI mice (Figure 2d-e). In addition, DermLef1KI mice have similar life spans as wild type
237 mice without any adverse effects (Supp Fig 3). Our results reveal that induced expression of Lef1
238 in fibroblasts does not negatively affect the development and homeostasis of murine skin.

239 Adult skin normally does not regenerate but has the capacity to reform non-functional hair
240 follicles (small and lack arrector pili) in wounds 1cm^2 or larger.(Ito et al., 2007) To test if
241 overexpression of Lef1 in adult dermal fibroblasts enhances hair regeneration in adult skin, we
242 wounded wild type (Lef1KI) and DermLef1KI mice at P24 with 1.2cm^2 wounds and harvested at
243 24dpw (Figure 4f). Our analysis comparing Lef1KI and DermLef1KI wound beds revealed
244 enhanced hair regeneration (Figure 4f-k). There were 5 times more regenerating hair follicles on
245 average in DermLef1KI wound beds compared to wild type wounds (Figure 4j-k). The non-
246 functional hair follicles that typically regenerate in large adult wounds are small and lack the
247 arrector pili, a smooth muscle that makes hair stand up when contracted. Strikingly, the hair
248 follicles regenerating in the DermLef1KI wound beds contained arrector pili (Figure 4i) and were
249 larger than hair follicles found in wild type wounds. This extensive ability to regenerate has only
250 been reported to occur in the African Spiny Mouse (Acomys) model.(Jiang et al., 2019; Seifert et
251 al., 2012) We conclude that Lef1 expression in dermal fibroblasts primes skin to enhances
252 regeneration.

253 **Dermal Lef1 transforms scarring wounds to be regenerative**

254 Wound healing studies utilize a standardized approach to take into account the hair follicle
255 cycle, which influences the wound healing process.(Ansell et al., 2011) Consequently, the bulk of
256 wound healing and regeneration studies are performed at 3 weeks of age (~P21) or at 7-8 weeks
257 of age (~P57) (Gay et al., 2013; Guerrero-Juarez et al., 2019; Ito et al., 2007; Lim et al., 2018;
258 Plikus et al., 2017; Plikus et al., 2008). In addition, a standard size wound of roughly 8mm in
259 diameter or smaller is used, which heal by scarring (Driskell et al., 2013; Lim et al., 2018; Rognoni
260 et al., 2016). Since Lef1KI mice showed enhanced regenerative capacity in large wounds, we
261 explored the regeneration potential of DermLef1KI skin, in wounds that normally scar. To
262 determine if the hair follicle cycle influences skin regeneration we performed wounds at different
263 time points. P24 which undergoes a hair follicle cycle during wound healing. P40 which heals
264 during the resting phase of the hair cycle. And P90 which is the beginning of the un-synchronized
265 hair follicle cycling that occurs in adult mice (Figure 5a). Scars formed in wounds performed at
266 P24 in both WT and DermLef1KI mice (Figure 5b-c,l). However, hair follicle regeneration with
267 arrector pili occurred in wounds performed at P40 and P90 in DermLef1KI mice (Figure 5d-k, l,
268 Supp Fig 4) (Figure 4h-k). We conclude that Lef1 expression in fibroblasts induces skin to support
269 hair follicle regeneration in wounds that heal outside of the hair follicle cycle.

270 Our wound healing studies mirror previous work suggesting that the size of a wound can
271 dictate the potential of skin to regenerate instead of scar (Ito et al., 2007). To explain 'why size
272 matters' we investigated and mapped the timing of wound closure and regeneration in the
273 context of molecular signals within the dermal macro-environment that are dynamically
274 changing throughout the hair follicle cycle (Plikus et al., 2008; Wang et al., 2017). Previous
275 studies have defined the activators and inhibitors that regulate hair follicle cycling during this
276 time (Wang et al., 2017) (Supp Table 3). Activators include the Wnt signaling pathway, Noggin,
277 Tgfb, and fibroblast markers such as PDGFRa. Inhibitors include the BMP signaling pathway.

278 These activators and inhibitors have been previously shown to modulate Lef1 activity (Jamora
279 et al., 2003). To explain why DermLef1KI mice scar at P24, we generated a diagram of wound
280 re-epithelization and healing time points comparing 8mm circular wounds to 1.2cm^2 wound in
281 the context of gene expression for inhibitors and activators at all time points during the hair
282 follicle cycle (Figure 5l). 8mm circular wounds re-epithelialize 7dpw (Driskell et al., 2013) in a
283 macro-environment with high levels of Lef1 inhibitors, which are not inductive to hair follicle
284 formation (Figure 5l). In contrast, large 1.2cm^2 wounds re-epithelialize during the time point of
285 the hair cycle that has high activators and low inhibitors (Figure 5l). We conclude that the size of
286 a wound dictates the time point as to when a wound closure is associated with inhibitor or
287 inductive regenerative signals.

288 **Discussion**

289 It is well established that embryonic and neonatal skin has the potential to heal in a scar-
290 less manner (Seifert et al., 2012). However, the cell types and signals that can transfer this ability
291 to adult skin have not been identified. In this study we identify Developing papillary fibroblasts as
292 a transient cell population that is defined by Lef1 expression. Inducing Lef1 expression in adult
293 fibroblasts will prime skin to support enhanced hair follicle regeneration. Interestingly, ectopic Lef1
294 expression in fibroblasts did not result in any adverse phenotypes with phenotypically normal mice
295 (Supp Fig 3).

296 scRNA-seq has provided an unprecedented insight in the cell types and molecular
297 pathways that are represented within regenerating and scarring wounds (Guerrero-Juarez et al.,
298 2019; Haensel et al., 2020; Joost et al., 2018). For example, comparisons of these different
299 repairing conditions have identified the activation of the Shh pathway as a key pathway to support
300 hair follicle regeneration in wounds of different sizes (Lim et al., 2018). However, the activation of
301 ectopic Shh in either the epidermis or dermis is associated with unwanted phenotypes and cancer
302 (Fan et al., 1997; Grachtchouk et al., 2000; Oro et al., 1997; Sun et al., 2020). Unexpectedly, we

303 discovered a transient papillary fibroblast population that is defined by Lef1 expression in
304 Developing skin instead of in Regenerating conditions. Importantly, our comparative analysis of
305 Regenerating and Scarring wounds reveals their similarities (Figure 1i) more than their differences
306 suggesting that the wound environment is a powerful driving force for gene expression even in a
307 heterogeneous population of cells. Consequently, the basic mechanisms occurring during
308 development and maintenance of neonatal tissue may hold the keys to transforming adult tissue
309 to regenerate instead of scarring.

310 Studies involving the activation of the Wnt and β-catenin pathways in skin have led to
311 important discoveries in wound healing research, but have produced contrasting results in the
312 context of fibroblast biology and hair follicle formation (Chen et al., 2012; Hamburg-Shields et al.,
313 2015; Ito et al., 2007; Lim et al., 2018; Mastrogiannaki et al., 2016; Rognoni et al., 2016). The
314 activation of β-catenin in fibroblasts during wound healing has been shown to inhibit hair follicle
315 reformation in scars (Lim et al., 2018; Rognoni et al., 2016). In contrast, the activation of β-catenin
316 during development increases hair formation and size (Chen et al., 2012; Enshell-Seijffers et al.,
317 2010). One explanation for these conflicting results is the presence of different fibroblast lineages
318 present in either development or wounds, which express different Lef/Tcf factors to direct a Wnt/β-
319 catenin specific response (Driskell et al., 2013; Philippeos et al., 2018; Rognoni et al., 2016). We
320 and others have shown that Lef1 is expressed in embryonic and neonatal papillary fibroblasts,
321 which is lost in adult fibroblasts (Driskell et al., 2013; Mastrogiannaki et al., 2016; Philippeos et
322 al., 2018; Rognoni et al., 2016). Here we demonstrate that Lef1 is a key inductive element in
323 developing fibroblasts that supports hair follicle formation in adult wounds. Our data indicates that
324 Lef1 expression in fibroblasts primes a response to Wnt signals to support hair follicle neogenesis
325 and arrector pili reformation, without negative affects to development or homeostasis, as seen in
326 other models (Seifert et al., 2012). Our results align with studies that induced Lef1 expression in
327 cultured human dermal papilla cells to enhance hair follicle formation in vitro (Abaci et al., 2018).

328 In humans, at the age of 50, the quality of the papillary dermis gradually deteriorates, which
329 correlates with decreased wound healing abilities (Haydont et al., 2019; Marcos-Garces et al.,
330 2014). Our data suggests that activating the human papillary region to retain its identity by
331 expression of Lef1 has the potential to enhance wound healing in humans.

332

333 **Material and Methods**

334 **Mouse models.** All mice were outbred on a C57BL6/CBA background, with male and female
335 mice used in all experiments. The following transgenic mouse lines were used in this study,
336 Twist2-Cre (Cat# 008712). The ROSA26-CAG-flox-GFP-STOP-flox-Lef1 and Lef1-flox-Exon7,8-
337 flox mouse has been previously described (Lynch et al., 2016; Yu et al., 2012). Wild type mice
338 utilized in scRNA-seq experiments were an outbred background of C57BL6/CBA mice.

339 **Wounding experiments.** All wounding experiments were done in accordance with the guidelines
340 from approved protocols Washington State University IACUC. Mice were wounded at post-natal
341 day (P) 2, P24, P40 and P90 as stated in the results section. All wounding experiments were
342 carried out with mice under anesthetization. The dorsal hair was shaved, and wounding areas
343 were disinfected. For full-thickness circular wound, 2mm and 8mm punch biopsy and surgical
344 scissors were used on P2 and P24/P40 mice, respectively. For large wounds, 1.44cm2 (1.2 x 1.2
345 cm) squares were excised using surgical scissors. Wounds were harvested at 7 dpw, 14 dpw, 24
346 dpw, and 30 dpw.

347 **Horizontal whole mount**. This procedure was described in Salz et al., 2017 (Salz and Driskell,
348 2017). Briefly, full thickness skin samples were collected and fixed in 4% Paraformaldehyde
349 (PFA), before being frozen in OCT compound in cryo-block. Samples were sectioned using
350 cryostat at 60 mm thickness. Skin sections were then stained with primary antibodies at 4C

351 overnight in PB buffer and with secondary antibodies in PB buffer for one hour. Samples were
352 mounted on glass cover slip with glycerol as mounting medium.

353 **Single Cell RNA Sequencing.** Cells isolation procedure was previously described in Jensen and
354 Driskell 2009 (Jensen et al., 2010). Single-cell cDNA libraries were prepared using the 10X
355 Genomics Chromium Single Cell 3' kit according to the company's instruction. The prepared
356 libraries were sequenced on Illumina HiSeq 4000. Sequencing data were processed by
357 CellRanger package. Downstream analysis was performed using published packages including
358 Scanpy, Scvelo, Velocyto. The analysis pipeline is published on the Driskell lab Github webpage
359 in Jupyter Notebook (https://github.com/DriskellLab/Priming-Skin-to-Regenerate-by-Inducing-
360 Lef1-Expression-in-Fibroblasts-).

361 **Microarray analysis.** The microarray data were previously published (GEO GSE11186) (Lin et
362 al., 2009). RMA normalization was used, and the bottom twentieth percentile of genes were
363 excluded from the analysis.

364 **Acknowledgements**

365 This work was supported by WSU New Faculty Seed Grant 2428-9926. The authors would like to
366 acknowledge Sean Thompson, Jonathan Jones, Kai Kretzschmar, and Klaas Mulder for their
367 discussion and help. The authors would also like to acknowledge the Washington State University
368 Franceschi Microscopy Imaging Center for the continued support in microscopic imaging.

369 **Author Contributions**

370 QP performed and designed the experiments, analyzed the data, and co-wrote the manuscript.
371 GF, LS, GGH, BW, and IMD assisted in performing and designing experiments. RRD conceived
372 of the project, assisted in experimental design, performed data analysis, and co-wrote the
373 manuscript.

374

Figure and Legends

Figure 1: Phan et al. 2020

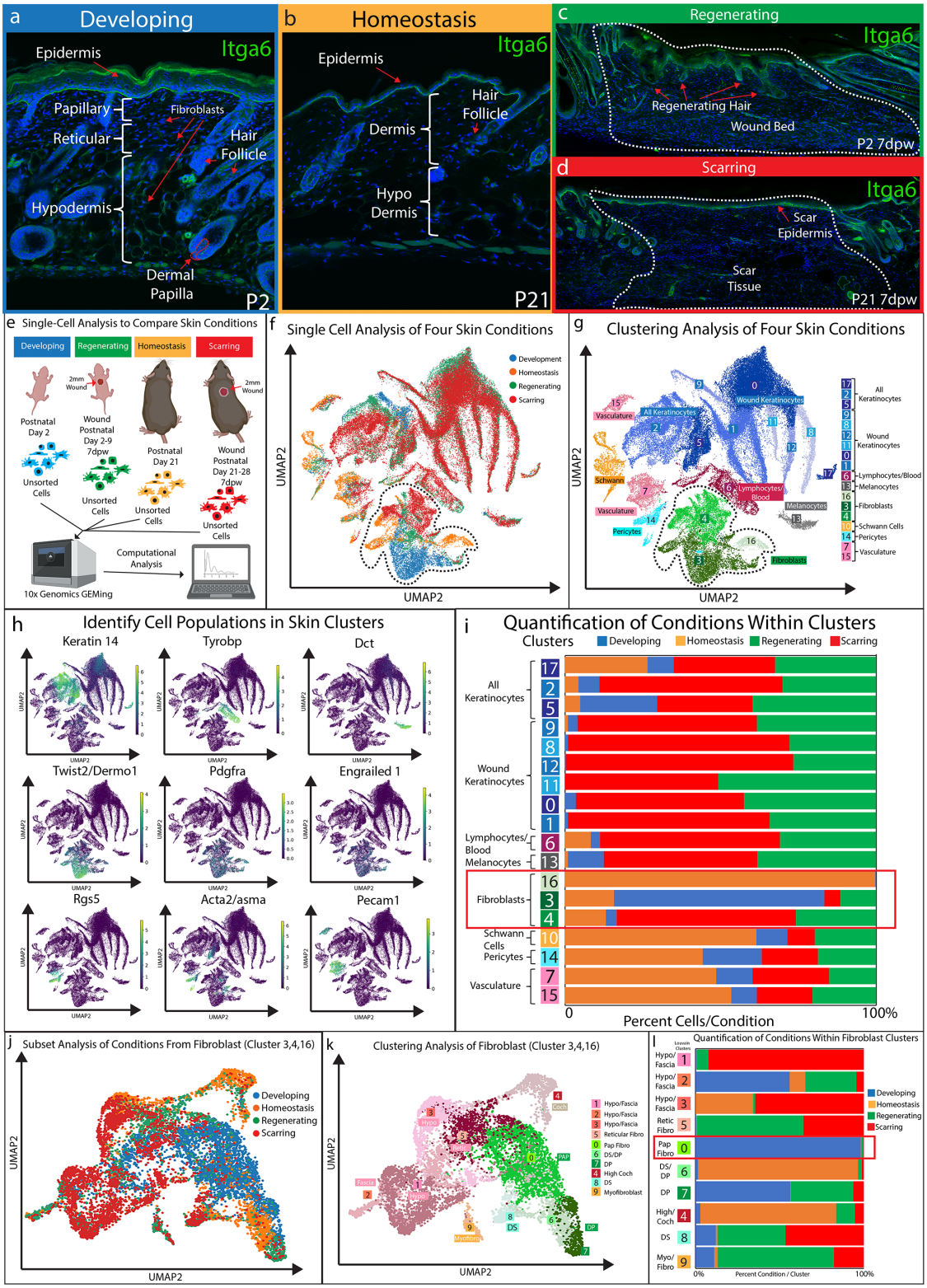

377 **Figure 1: Fibroblasts in Developing skin are distinct from Regenerating, Scarring, and**
378 **Homeostatic Conditions.** (a-d) Immunostaining analysis and histological map of the dermis in
379 Developing Post-natal day 2 (P2) skin (a), Homeostatic skin at P21 (b), skin undergoing
380 regeneration P2 7 days post wound (7dwp) (c), and skin repairing a wound via scarring P21 7dpw
381 (d). (e) Schematic representation of single cell isolation, library preparation, and sequencing
382 analysis for unsorted cells from Developing (P2), Regenerating (P2 7dpw), Homeostatic (P21),
383 and Scarring (P21 7dpw) conditions. (f) UMAP visualization of all cell populations for all
384 conditions. Each cell is color coded based according to condition as labeled. (g) Clustering
385 analysis of the UMAP plot, color coded based on cell types. (h) Overlaying gene expression on
386 UMAP clusters to identify cell types. (i) Quantification of the percentage of all cells represented
387 within a cluster. (j) Subset and re-clustering of Cluster 3,4,16 by computational integration. (k)
388 Cluster analysis of integrated fibroblast clusters 3,4,16. (l) Quantitation of fibroblasts within each
389 cluster represented by condition.

Figure 2: Phan et al. 2020

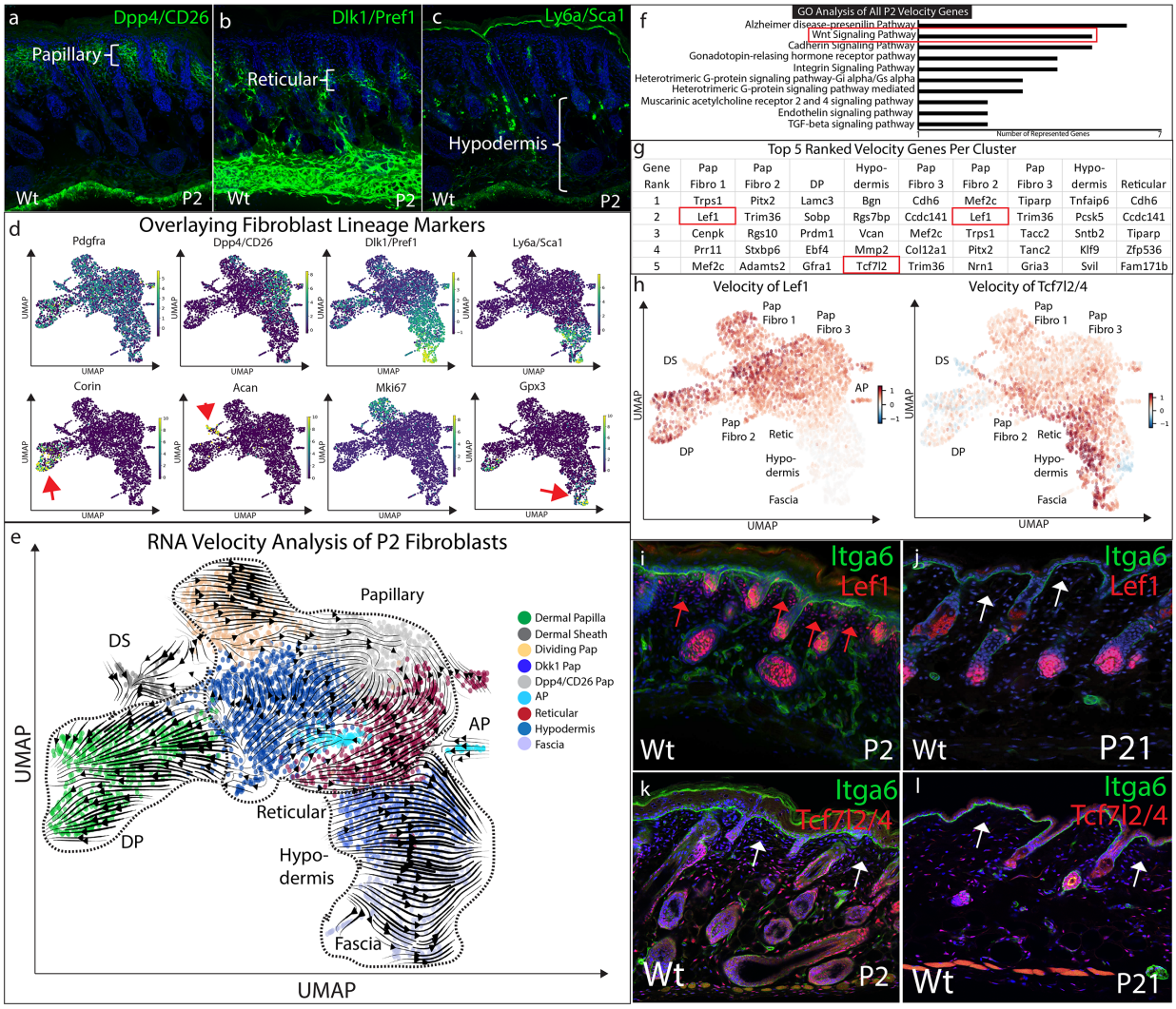

Figure 2: Papillary fibroblast lineage trajectory is defined by Lef1 in RNA Velocity analysis. (a-c) Immunostaining Development (P2) skin for Papillary (a) (Dpp4/CD26), Reticular/Hypodermal (b) (Dlk1/Pref1), and Hypodermal makers (c) (Ly6a/Sca1). (d) Overlaying fibroblast lineage markers on UMAP projections of Developing fibroblasts. (e) RNA Velocity analysis over layed on UMAP projection of clustered fibroblasts. Clusters are colored coded and labeled. (f) GO Analysis of 195 driver genes of RNA Velocity for Developing fibroblasts. (g) Top 5 Velocity driver genes of Developing fibroblast clusters. (h) Overlaying Lef1 and Tcf7l2/4 velocity on UMAP projections of Developmental fibroblast. (i-l) Immunostaining Developing (P2) and

399 Homeostatic (P21) time points for Lef1 and Tcf7l2/4 expression and counterstained with Itga6.
400 Red arrows indicate areas of papillary dermis expressing Lef1. White arrows indicate papillary
401 dermal region.

Figure 3: Phan et al. 2020

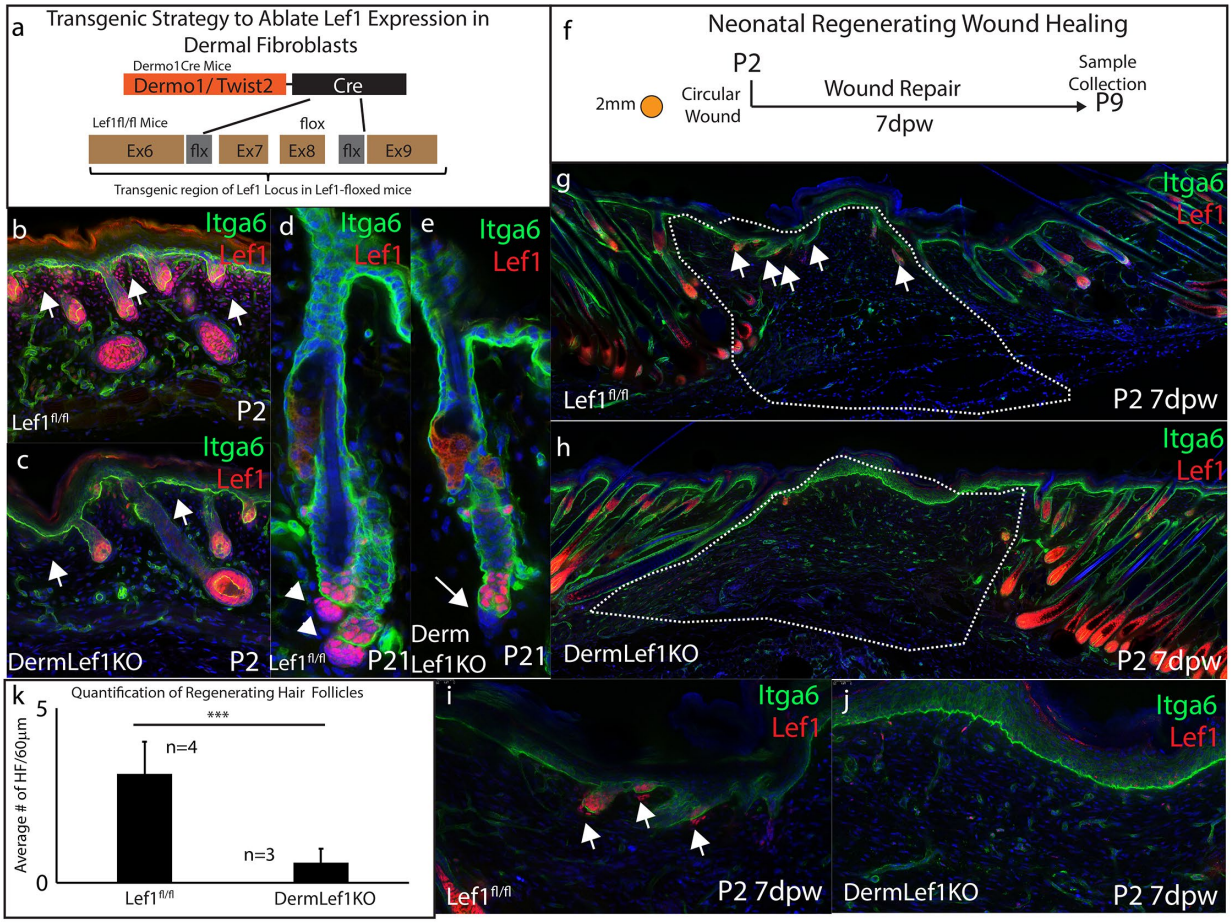

402

403 **Figure 3: Dermal Lef1 is required to support hair follicle regeneration in neonatal wounds.**
404 (a) Schematic representation of transgenic strategy to ablate Lef1 expression in dermal
405 fibroblasts. (b-e) Verifying dermal Lef1 ablation by immunostaining. White arrows indicate
406 papillary regions (b-c) or dermal papilla (d-e). (f) Schematic describing 2mm circular wounds and
407 harvest times to test if dermal Lef1 is required for regeneration. (g-i) Immunostaining of P2 7 days
408 post wound (7dpw) skin for Itga6 and Lef1. Wound beds are highlighted by white outline. White

arrows indicate regenerating hair follicles. (k) Quantification of regenerating hair follicles in wounds beds of n=4 Lef1fl/fl (wt) and n=3 DermLef1KO mice. $p < 0.003$

Figure 4: Phan et al. 2020

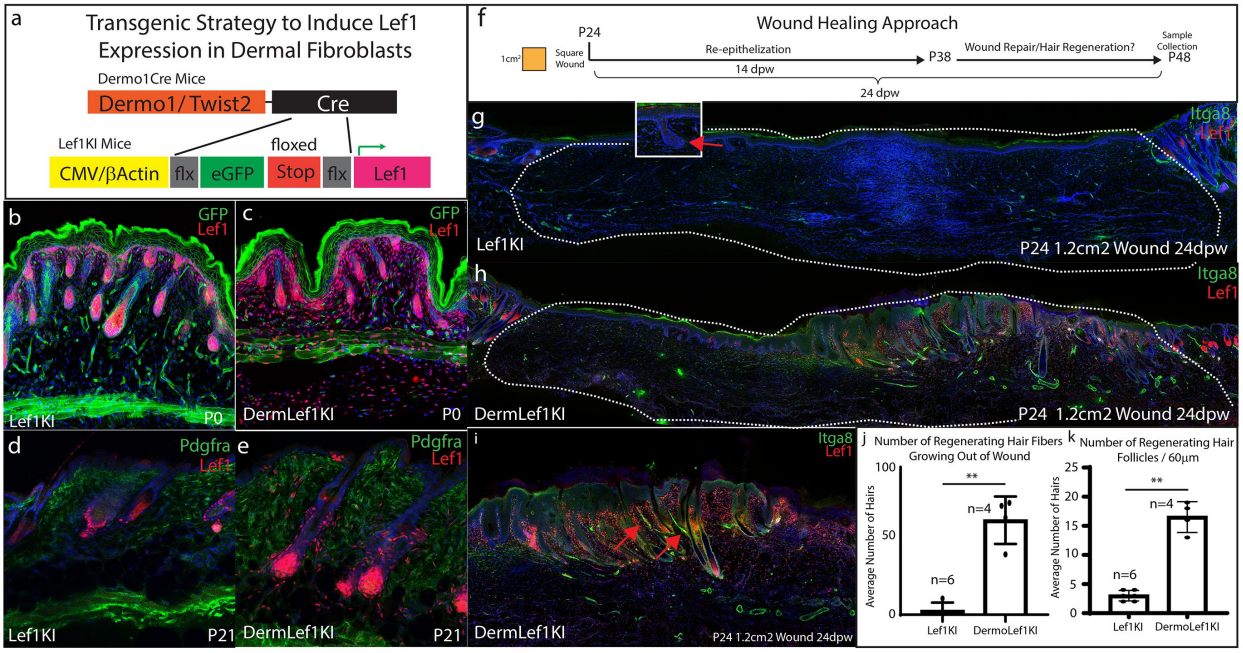

Figure 4: Lef1 expression in dermal fibroblast enhances skin regeneration in large wounds. (a) Schematic representation of transgenic strategy to ectopically express Lef1 in fibroblasts during development, homeostasis and wound healing. (b-c) Immunostaining for Lef1 and GFP in P0 Lef1KI and DermLef1KI (Dermo1Cre+/Lef1KI+) mice. (d-e) Immunostaining for Lef1 and PDGFRa in P21 Lef1KI and DermLef1KI mice. (f) Schematic representation of wound healing approach. (g-k) Immunostaining tissue for Lef1 and Itga8 (arrector pili) from the wounds of Lef1KI and DermLef1KI mice. Regenerating hair follicles in Lef1KI mice can be found by red arrows. Wound beds are marked by red squares. High resolution area of regenerating hair follicles in DermLef1Ki mice (i). (j) Quantification of regenerating hair follicles growing out of the wound beds of Lef1KI n=6 and DermLef1KI n=4 mice $p < 0.004$. (k) Quantification of regenerating hair follicles detected in 60 μm sections of wound beds. $p < 0.001$

Figure 5: Phan et al. 2020

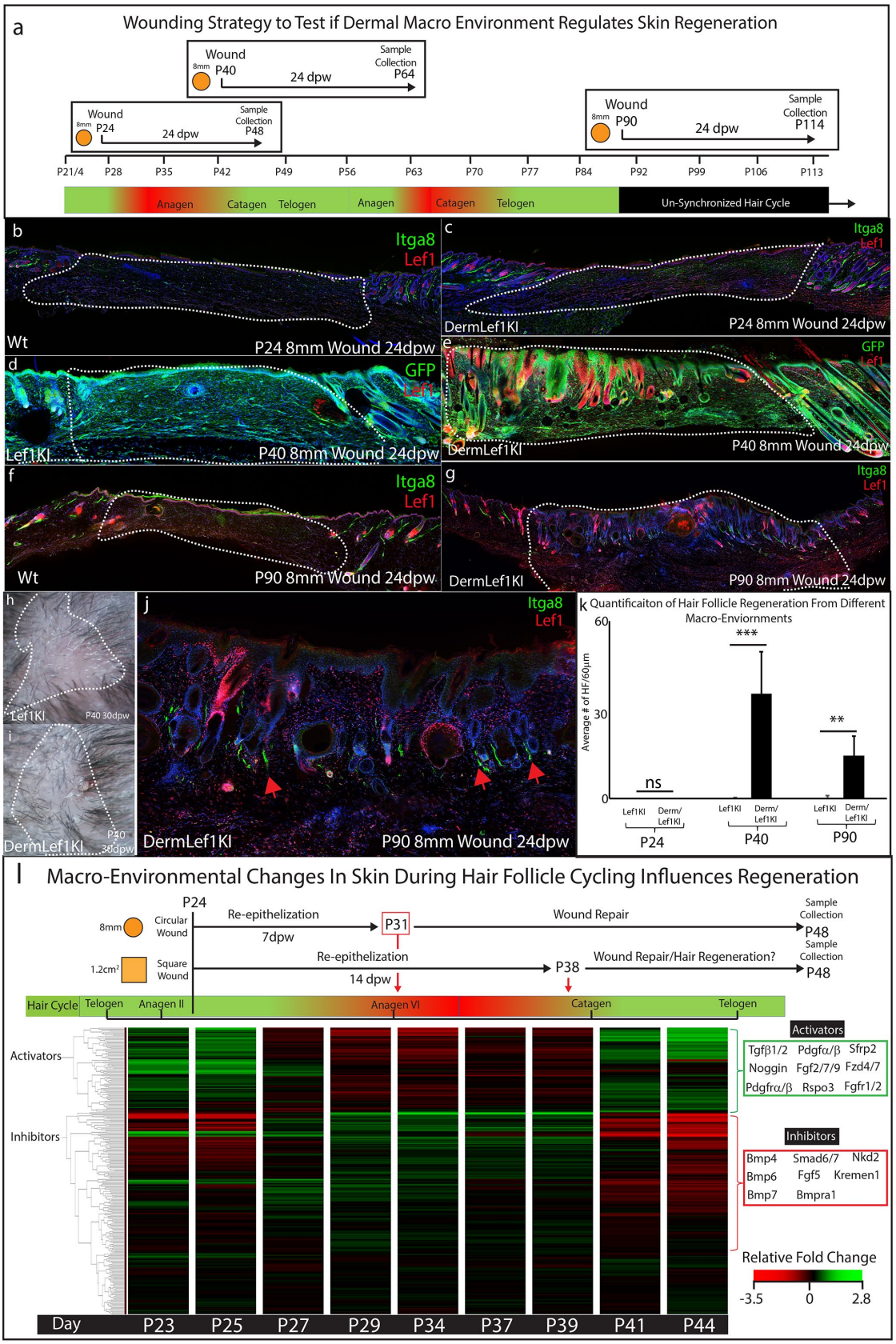

423

Figure 5: Lef1 expression in dermal fibroblasts enhances skin regeneration in permissive macro environments. (a) Schematic of the differential wound healing analysis from different time points of the hair follicle cycle in murine skin. (b-g,j) Immunostaining analysis of wounds 24dpw from P24 (b-d), P40 (d-e), and P90 (f-g,j). Sections were stained for either Itga8 and Lef1 (b-c,f-g,j) or GFP and Lef1 (d-e). Itga8 labels arrector pili. (h-i) Macroscopic analysis of wound beds from Wt (Lef1KI) and DermLef1KI mice. Hair follicles could be seen growing out of the wound bed of DermLef1KI mice. (k) Quantification of the average number of regenerating hair follicles detected in wounds beds of 60 μm sections from P24 (ns) 24dpw ($p < 0.0009$), P40 24dpw, and P90 24dpw ($p < 0.007$). (l) Schematic representation of different wound healing approaches above a heatmap of microarray data (Lin et al., 2009) from key time points during hair follicle cycling. Heatmap is generated from a list of Activator and Inhibitor genes reported to regulate the progression of the hair follicle cycle (Wang et al., 2017).

Supp Fig1: Phan et al. 2020

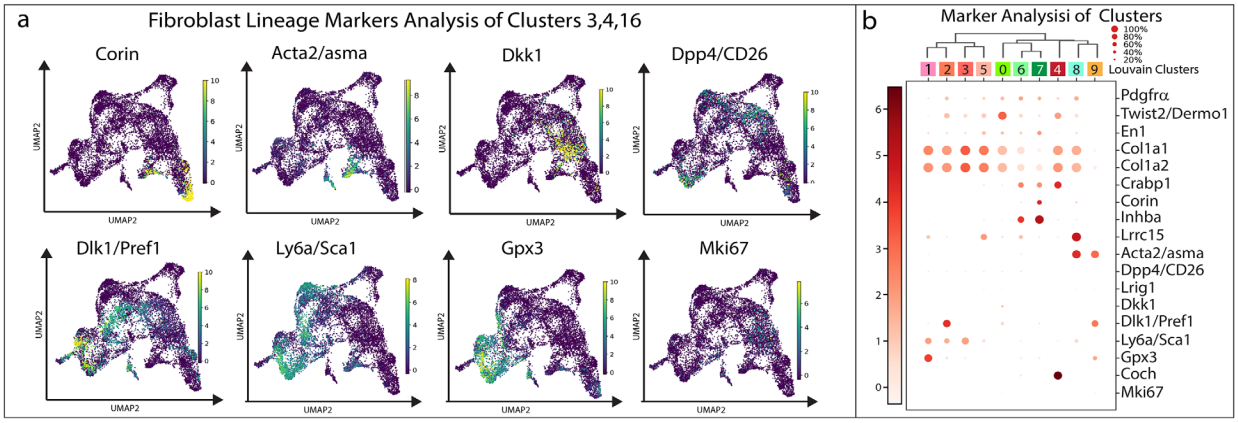

Supplemental Figure 1: Classifying fibroblast clusters and conditions in Development, Regeneration, Scarring, and Homeostasis. (a) Over-laying gene expression for cell markers on UMAP plots. (b) Dotplot of genes based on expression in cluster.

Supp Fig 2: Phan et al. 2020

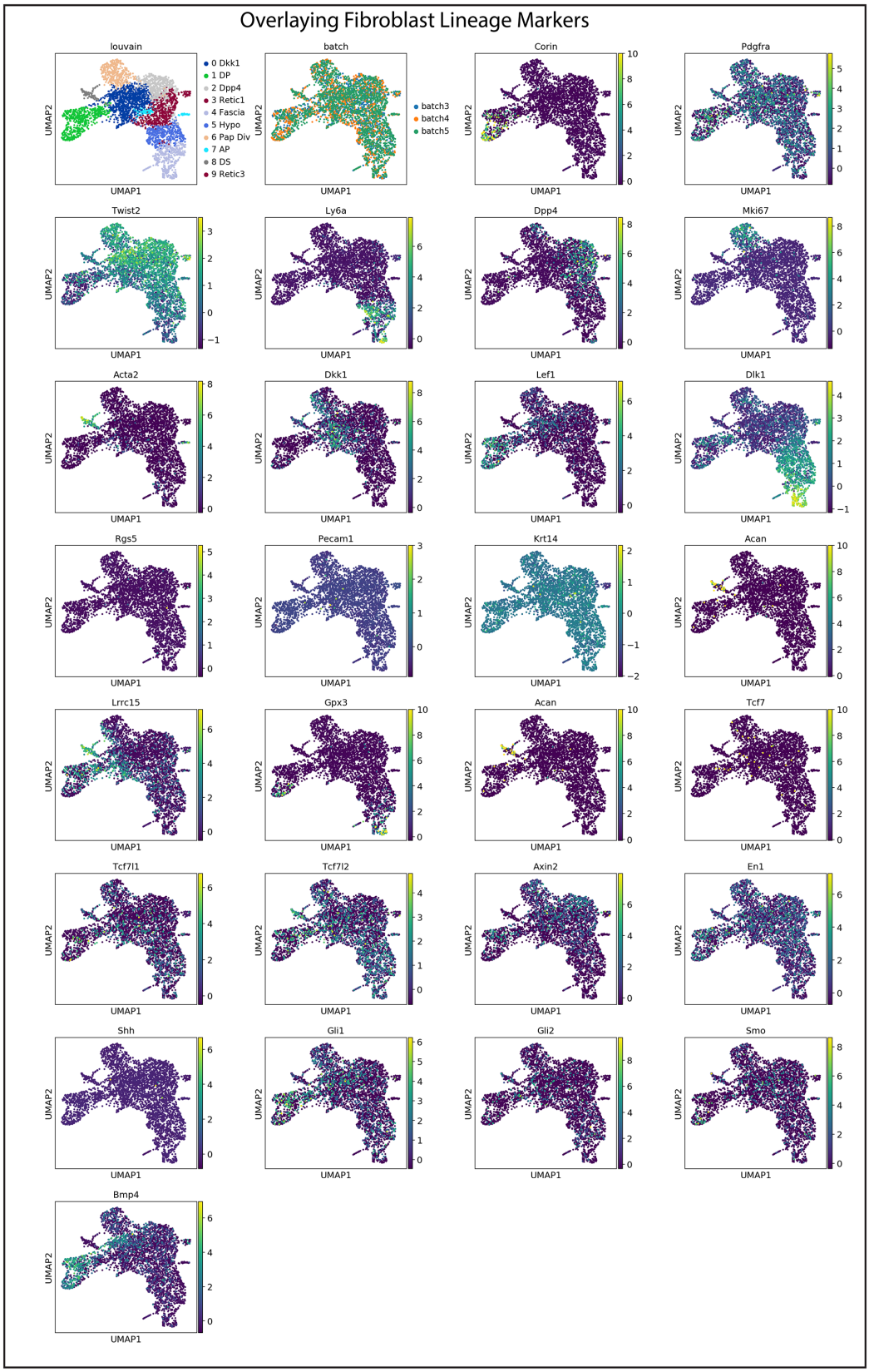

441

442 **Supplemental Figure 2: Classifying fibroblast clusters in Developing fibroblasts.** (a) Over-
443 laying gene expression for fibroblast lineage markers.

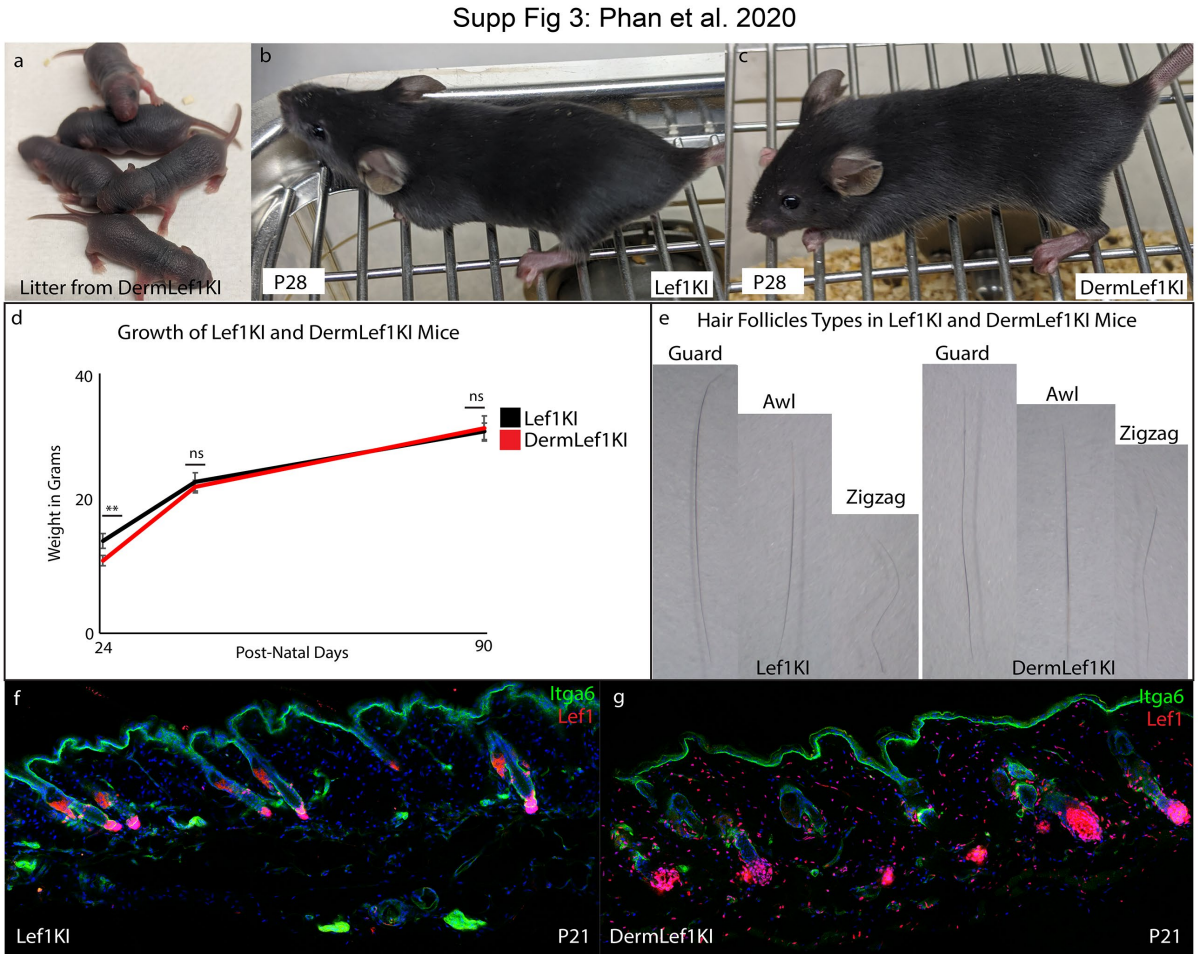

444

445 **Supplemental Figure 3: DermLef1KI mice does not show overt phenotypic variations.** (a)
446 Images of P4 litter from DermLef1KI mice revealing viability of line. (b-c) P28 of wild type (b) and
447 DermLef1KI (c) mice. (d) The growth curve of Wt (Lef1KI) mice compared to DermLef1KI mice at
448 P24, P40, and P90. P24 $p < 0.005$. (e) Macroscopic images of different hair follicle types from Wt
449 (Lef1KI) and DermLef1KI hair follicles. (f-g) Immunostaining analysis of sections from P21 skin
450 from Wt (Lef1KI) and DermLef1KI mice stained for Itga6 and Lef1.

Supp Fig 4: Phan et al. 2020

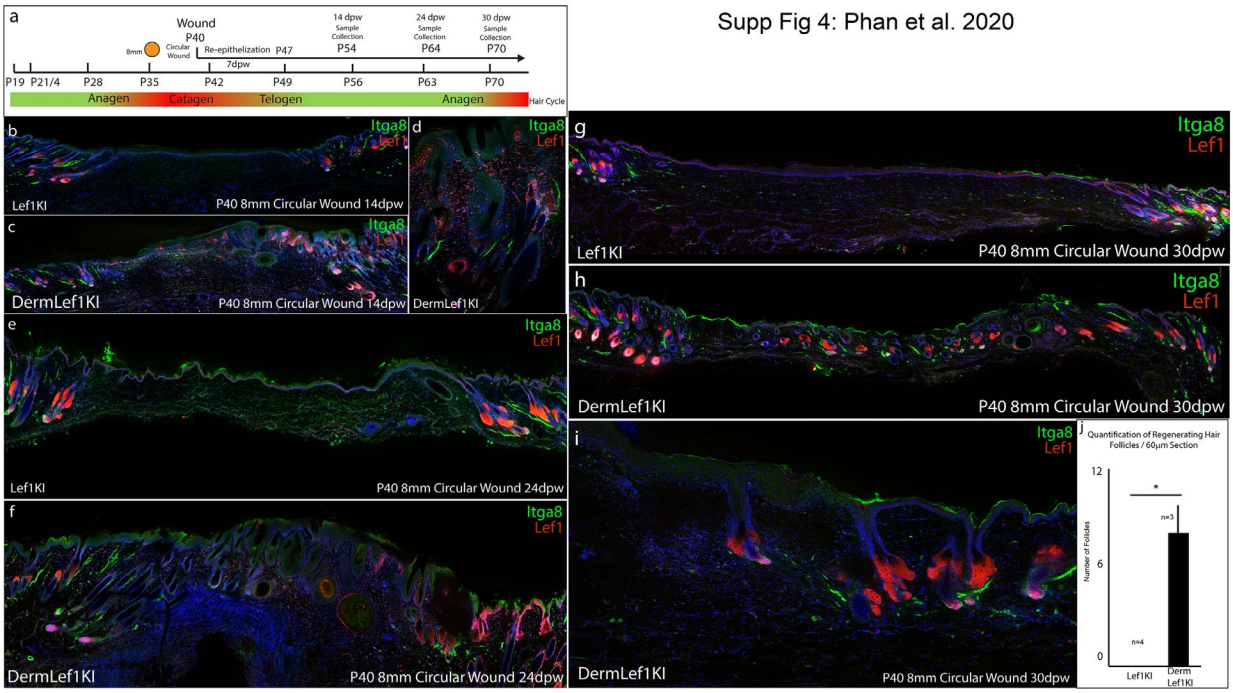

Supplemental Figure 4: Analysis of the regenerative potential of DermLef1KI wounds at P40. (a) Schematic describing the wounding and tissue collection strategy. (b-j) Immunostaining analysis of wild type (Lef1KI) and DermLef1KI mice wounded at P40 and collected at 14 dpw (b-d), 24dpw (e-f), and 30dpw (g-i). All sections were immunostained for Itga8 and Lef1. (j) Quantification of hair follicles in 60µm sections of Wt (Lef1KI) and DermLef1KI skin 30dpw. $p < 0.04$

460 **Bibliography**

461 Abaci, H.E., Coffman, A., Doucet, Y., Chen, J., Jackow, J., Wang, E., Guo, Z., Shin, J.U., Jahoda, C.A., and
462 Christiano, A.M. (2018). Tissue engineering of human hair follicles using a biomimetic developmental
463 approach. Nat Commun *9*, 5301.
464 Adam, R.C., Yang, H., Ge, Y., Lien, W.H., Wang, P., Zhao, Y., Polak, L., Levorse, J., Baksh, S.C., Zheng, D.*, et*
465 *al.* (2018). Temporal Layering of Signaling Effectors Drives Chromatin Remodeling during Hair Follicle
466 Stem Cell Lineage Progression. Cell Stem Cell *22*, 398-413 e397.
467 Ansell, D.M., Kloepper, J.E., Thomason, H.A., Paus, R., and Hardman, M.J. (2011). Exploring the "hair
468 growth-wound healing connection": anagen phase promotes wound re-epithelialization. J Invest
469 Dermatol *131*, 518-528.
470 Chen, D., Jarrell, A., Guo, C., Lang, R., and Atit, R. (2012). Dermal beta-catenin activity in response to
471 epidermal Wnt ligands is required for fibroblast proliferation and hair follicle initiation. Development
472 *139*, 1522-1533.
473 Chen, J.S., Longaker, M.T., and Gurtner, G.C. (2013). Murine models of human wound healing. Methods
474 Mol Biol *1037*, 265-274.
475 Collins, C.A., Kretzschmar, K., and Watt, F.M. (2011). Reprogramming adult dermis to a neonatal state
476 through epidermal activation of beta-catenin. Development *138*, 5189-5199.
477 Correa-Gallegos, D., Jiang, D., Christ, S., Ramesh, P., Ye, H., Wannemacher, J., Kalgudde Gopal, S., Yu, Q.,
478 Aichler, M., Walch, A.*, et al.* (2019). Patch repair of deep wounds by mobilized fascia. Nature *576*, 287-
479 292.
480 Driskell, R.R., Lichtenberger, B.M., Hoste, E., Kretzschmar, K., Simons, B.D., Charalambous, M., Ferron,
481 S.R., Herault, Y., Pavlovic, G., Ferguson-Smith, A.C.*, et al.* (2013). Distinct fibroblast lineages determine
482 dermal architecture in skin development and repair. Nature *504*, 277-281.
483 Driskell, R.R., and Watt, F.M. (2015). Understanding fibroblast heterogeneity in the skin. Trends Cell Biol
484 *25*, 92-99.
485 Enshell-Seijffers, D., Lindon, C., Kashiwagi, M., and Morgan, B.A. (2010). beta-catenin activity in the
486 dermal papilla regulates morphogenesis and regeneration of hair. Dev Cell *18*, 633-642.
487 Enshell-Seijffers, D., Lindon, C., and Morgan, B.A. (2008). The serine protease Corin is a novel modifier of
488 the Agouti pathway. Development *135*, 217-225.
489 Fan, H., Oro, A.E., Scott, M.P., and Khavari, P.A. (1997). Induction of basal cell carcinoma features in
490 transgenic human skin expressing Sonic Hedgehog. Nat Med *3*, 788-792.
491 Gay, D., Kwon, O., Zhang, Z., Spata, M., Plikus, M.V., Holler, P.D., Ito, M., Yang, Z., Treffeisen, E., Kim,
492 C.D.*, et al.* (2013). Fgf9 from dermal gammadelta T cells induces hair follicle neogenesis after wounding.
493 Nat Med *19*, 916-923.
494 Ge, Y., Miao, Y., Gur-Cohen, S., Gomez, N., Yang, H., Nikolova, M., Polak, L., Hu, Y., Verma, A., Elemento,
495 O.*, et al.* (2020). The aging skin microenvironment dictates stem cell behavior. Proc Natl Acad Sci U S A
496 *117*, 5339-5350.
497 Grachtchouk, M., Mo, R., Yu, S., Zhang, X., Sasaki, H., Hui, C.C., and Dlugosz, A.A. (2000). Basal cell
498 carcinomas in mice overexpressing Gli2 in skin. Nat Genet *24*, 216-217.
499 Guerrero-Juarez, C.F., Dedhia, P.H., Jin, S., Ruiz-Vega, R., Ma, D., Liu, Y., Yamaga, K., Shestova, O., Gay,
500 D.L., Yang, Z.*, et al.* (2019). Single-cell analysis reveals fibroblast heterogeneity and myeloid-derived
501 adipocyte progenitors in murine skin wounds. Nat Commun *10*, 650.
502 Haensel, D., Jin, S., Sun, P., Cinco, R., Dragan, M., Nguyen, Q., Cang, Z., Gong, Y., Vu, R., MacLean, A.L.*, et*
503 *al.* (2020). Defining Epidermal Basal Cell States during Skin Homeostasis and Wound Healing Using
504 Single-Cell Transcriptomics. Cell Rep *30*, 3932-3947 e3936.

505 Hamburg-Shields, E., DiNuoscio, G.J., Mullin, N.K., Lafyatis, R., and Atit, R.P. (2015). Sustained beta-
506 catenin activity in dermal fibroblasts promotes fibrosis by up-regulating expression of extracellular
507 matrix protein-coding genes. J Pathol *235*, 686-697.
508 Haydont, V., Bernard, B.A., and Fortunel, N.O. (2019). Age-related evolutions of the dermis: Clinical
509 signs, fibroblast and extracellular matrix dynamics. Mech Ageing Dev *177*, 150-156.
510 Heitman, N., Sennett, R., Mok, K.W., Saxena, N., Srivastava, D., Martino, P., Grisanti, L., Wang, Z.,
511 Ma'ayan, A., Rompolas, P.*, et al.* (2020). Dermal sheath contraction powers stem cell niche relocation
512 during hair cycle regression. Science *367*, 161-166.
513 Hu, M.S., Borrelli, M.R., Hong, W.X., Malhotra, S., Cheung, A.T.M., Ransom, R.C., Rennert, R.C., Morrison,
514 S.D., Lorenz, H.P., and Longaker, M.T. (2018). Embryonic skin development and repair. Organogenesis
515 *14*, 46-63.
516 Ito, M., Yang, Z., Andl, T., Cui, C., Kim, N., Millar, S.E., and Cotsarelis, G. (2007). Wnt-dependent de novo
517 hair follicle regeneration in adult mouse skin after wounding. Nature *447*, 316-320.
518 Jamora, C., DasGupta, R., Kocieniewski, P., and Fuchs, E. (2003). Links between signal transduction,
519 transcription and adhesion in epithelial bud development. Nature *422*, 317-322.
520 Jensen, K.B., Driskell, R.R., and Watt, F.M. (2010). Assaying proliferation and differentiation capacity of
521 stem cells using disaggregated adult mouse epidermis. Nat Protoc *5*, 898-911.
522 Jiang, D., Correa-Gallegos, D., Christ, S., Stefanska, A., Liu, J., Ramesh, P., Rajendran, V., De Santis, M.M.,
523 Wagner, D.E., and Rinkevich, Y. (2018). Two succeeding fibroblastic lineages drive dermal development
524 and the transition from regeneration to scarring. Nat Cell Biol *20*, 422-431.
525 Jiang, T.X., Harn, H.I., Ou, K.L., Lei, M., and Chuong, C.M. (2019). Comparative regenerative biology of
526 spiny (Acomys cahirinus) and laboratory (Mus musculus) mouse skin. Exp Dermatol *28*, 442-449.
527 Johnston, A.P., Naska, S., Jones, K., Jinno, H., Kaplan, D.R., and Miller, F.D. (2013). Sox2-mediated
528 regulation of adult neural crest precursors and skin repair. Stem Cell Reports *1*, 38-45.
529 Joost, S., Annusver, K., Jacob, T., Sun, X., Dalessandri, T., Sivan, U., Sequeira, I., Sandberg, R., and Kasper,
530 M. (2020). The Molecular Anatomy of Mouse Skin during Hair Growth and Rest. Cell Stem Cell *26*, 441-
531 457 e447.
532 Joost, S., Jacob, T., Sun, X., Annusver, K., La Manno, G., Sur, I., and Kasper, M. (2018). Single-Cell
533 Transcriptomics of Traced Epidermal and Hair Follicle Stem Cells Reveals Rapid Adaptations during
534 Wound Healing. Cell Rep *25*, 585-597 e587.
535 Joost, S., Zeisel, A., Jacob, T., Sun, X., La Manno, G., Lonnerberg, P., Linnarsson, S., and Kasper, M.
536 (2016). Single-Cell Transcriptomics Reveals that Differentiation and Spatial Signatures Shape Epidermal
537 and Hair Follicle Heterogeneity. Cell Syst *3*, 221-237 e229.
538 Kaushal, G.S., Rognoni, E., Lichtenberger, B.M., Driskell, R.R., Kretzschmar, K., Hoste, E., and Watt, F.M.
539 (2015). Fate of Prominin-1 Expressing Dermal Papilla Cells during Homeostasis, Wound Healing and Wnt
540 Activation. J Invest Dermatol *135*, 2926-2934.
541 La Manno, G., Soldatov, R., Zeisel, A., Braun, E., Hochgerner, H., Petukhov, V., Lidschreiber, K., Kastriti,
542 M.E., Lonnerberg, P., Furlan, A.*, et al.* (2018). RNA velocity of single cells. Nature *560*, 494-498.
543 Lim, C.H., Sun, Q., Ratti, K., Lee, S.H., Zheng, Y., Takeo, M., Lee, W., Rabbani, P., Plikus, M.V., Cain, J.E.*, et*
544 *al.* (2018). Hedgehog stimulates hair follicle neogenesis by creating inductive dermis during murine skin
545 wound healing. Nat Commun *9*, 4903.
546 Lin, K.K., Kumar, V., Geyfman, M., Chudova, D., Ihler, A.T., Smyth, P., Paus, R., Takahashi, J.S., and
547 Andersen, B. (2009). Circadian clock genes contribute to the regulation of hair follicle cycling. PLoS
548 Genet *5*, e1000573.
549 Lo, D.D., Zimmermann, A.S., Nauta, A., Longaker, M.T., and Lorenz, H.P. (2012). Scarless fetal skin wound
550 healing update. Birth Defects Res C Embryo Today *96*, 237-247.

551 Lynch, T.J., Anderson, P.J., Xie, W., Crooke, A.K., Liu, X., Tyler, S.R., Luo, M., Kusner, D.M., Zhang, Y., Neff,
552 T.*, et al.* (2016). Wnt Signaling Regulates Airway Epithelial Stem Cells in Adult Murine Submucosal
553 Glands. Stem Cells *34*, 2758-2771.
554 Marcos-Garces, V., Molina Aguilar, P., Bea Serrano, C., Garcia Bustos, V., Benavent Segui, J., Ferrandez
555 Izquierdo, A., and Ruiz-Sauri, A. (2014). Age-related dermal collagen changes during development,
556 maturation and ageing - a morphometric and comparative study. J Anat *225*, 98-108.
557 Mastrogiannaki, M., Lichtenberger, B.M., Reimer, A., Collins, C.A., Driskell, R.R., and Watt, F.M. (2016).
558 beta-Catenin Stabilization in Skin Fibroblasts Causes Fibrotic Lesions by Preventing Adipocyte
559 Differentiation of the Reticular Dermis. J Invest Dermatol *136*, 1130-1142.
560 Mok, K.W., Saxena, N., Heitman, N., Grisanti, L., Srivastava, D., Muraro, M.J., Jacob, T., Sennett, R.,
561 Wang, Z., Su, Y.*, et al.* (2019). Dermal Condensate Niche Fate Specification Occurs Prior to Formation
562 and Is Placode Progenitor Dependent. Dev Cell *48*, 32-48 e35.
563 Muller-Rover, S., Handjiski, B., van der Veen, C., Eichmuller, S., Foitzik, K., McKay, I.A., Stenn, K.S., and
564 Paus, R. (2001). A comprehensive guide for the accurate classification of murine hair follicles in distinct
565 hair cycle stages. J Invest Dermatol *117*, 3-15.
566 Nguyen, H., Merrill, B.J., Polak, L., Nikolova, M., Rendl, M., Shaver, T.M., Pasolli, H.A., and Fuchs, E.
567 (2009). Tcf3 and Tcf4 are essential for long-term homeostasis of skin epithelia. Nat Genet *41*, 1068-1075.
568 Nusse, R., and Clevers, H. (2017). Wnt/beta-Catenin Signaling, Disease, and Emerging Therapeutic
569 Modalities. Cell *169*, 985-999.
570 Oro, A.E., Higgins, K.M., Hu, Z., Bonifas, J.M., Epstein, E.H., Jr., and Scott, M.P. (1997). Basal cell
571 carcinomas in mice overexpressing sonic hedgehog. Science *276*, 817-821.
572 Philippeos, C., Telerman, S.B., Oules, B., Pisco, A.O., Shaw, T.J., Elgueta, R., Lombardi, G., Driskell, R.R.,
573 Soldin, M., Lynch, M.D.*, et al.* (2018). Spatial and Single-Cell Transcriptional Profiling Identifies
574 Functionally Distinct Human Dermal Fibroblast Subpopulations. J Invest Dermatol *138*, 811-825.
575 Plikus, M.V., Guerrero-Juarez, C.F., Ito, M., Li, Y.R., Dedhia, P.H., Zheng, Y., Shao, M., Gay, D.L., Ramos,
576 R., Hsi, T.C.*, et al.* (2017). Regeneration of fat cells from myofibroblasts during wound healing. Science
577 *355*, 748-752.
578 Plikus, M.V., Mayer, J.A., de la Cruz, D., Baker, R.E., Maini, P.K., Maxson, R., and Chuong, C.M. (2008).
579 Cyclic dermal BMP signalling regulates stem cell activation during hair regeneration. Nature *451*, 340-
580 344.
581 Polanski, K., Young, M.D., Miao, Z., Meyer, K.B., Teichmann, S.A., and Park, J.E. (2020). BBKNN: fast
582 batch alignment of single cell transcriptomes. Bioinformatics *36*, 964-965.
583 Rinkevich, Y., Walmsley, G.G., Hu, M.S., Maan, Z.N., Newman, A.M., Drukker, M., Januszyk, M., Krampitz,
584 G.W., Gurtner, G.C., Lorenz, H.P.*, et al.* (2015). Skin fibrosis. Identification and isolation of a dermal
585 lineage with intrinsic fibrogenic potential. Science *348*, aaa2151.
586 Rognoni, E., Gomez, C., Pisco, A.O., Rawlins, E.L., Simons, B.D., Watt, F.M., and Driskell, R.R. (2016).
587 Inhibition of beta-catenin signalling in dermal fibroblasts enhances hair follicle regeneration during
588 wound healing. Development *143*, 2522-2535.
589 Salz, L., and Driskell, R.R. (2017). Horizontal Whole Mount: A Novel Processing and Imaging Protocol for
590 Thick, Three-dimensional Tissue Cross-sections of Skin. J Vis Exp.
591 Salzer, M.C., Lafzi, A., Berenguer-Llergo, A., Youssif, C., Castellanos, A., Solanas, G., Peixoto, F.O.,
592 Stephan-Otto Attolini, C., Prats, N., Aguilera, M.*, et al.* (2018). Identity Noise and Adipogenic Traits
593 Characterize Dermal Fibroblast Aging. Cell *175*, 1575-1590 e1522.
594 Schmidt, B.A., and Horsley, V. (2013). Intradermal adipocytes mediate fibroblast recruitment during skin
595 wound healing. Development *140*, 1517-1527.
596 Seifert, A.W., Kiama, S.G., Seifert, M.G., Goheen, J.R., Palmer, T.M., and Maden, M. (2012). Skin
597 shedding and tissue regeneration in African spiny mice (Acomys). Nature *489*, 561-565.

598 Sun, X., Are, A., Annusver, K., Sivan, U., Jacob, T., Dalessandri, T., Joost, S., Fullgrabe, A., Gerling, M., and
599 Kasper, M. (2020). Coordinated hedgehog signaling induces new hair follicles in adult skin. Elife *9*.
600 Telerman, S.B., Rognoni, E., Sequeira, I., Pisco, A.O., Lichtenberger, B.M., Culley, O., Viswanathan, P.,
601 Driskell, R.R., and Watt, F.M. (2017). Dermal Blimp1 acts downstream of epidermal TGFbeta and
602 Wnt/beta-catenin to regulate hair follicle formation and growth. J Invest Dermatol.
603 Walmsley, G.G., Maan, Z.N., Wong, V.W., Duscher, D., Hu, M.S., Zielins, E.R., Wearda, T., Muhonen, E.,
604 McArdle, A., Tevlin, R.*, et al.* (2015). Scarless wound healing: chasing the holy grail. Plast Reconstr Surg
605 *135*, 907-917.
606 Wang, Q., Oh, J.W., Lee, H.L., Dhar, A., Peng, T., Ramos, R., Guerrero-Juarez, C.F., Wang, X., Zhao, R.,
607 Cao, X.*, et al.* (2017). A multi-scale model for hair follicles reveals heterogeneous domains driving rapid
608 spatiotemporal hair growth patterning. Elife *6*.
609 Wolf, F.A., Angerer, P., and Theis, F.J. (2018). SCANPY: large-scale single-cell gene expression data
610 analysis. Genome Biol *19*, 15.
611 Yang, C.C., and Cotsarelis, G. (2010). Review of hair follicle dermal cells. J Dermatol Sci *57*, 2-11.
612 Yu, S., Zhou, X., Steinke, F.C., Liu, C., Chen, S.C., Zagorodna, O., Jing, X., Yokota, Y., Meyerholz, D.K.,
613 Mullighan, C.G.*, et al.* (2012). The TCF-1 and LEF-1 transcription factors have cooperative and opposing
614 roles in T cell development and malignancy. Immunity *37*, 813-826.

615